nature chemistry

SUPPLEMENTARY INFORMATION

DOI: 10.1038/NCHEM.2491

Experimental Realization of Two-dimensional Boron Sheets

Baojie Feng[1], Jin Zhang[1], Qing Zhong[1], Wenbin Li[1], Shuai Li[1], Hui Li[1], Peng Cheng[1], Sheng Meng[1,2], Lan Chen[1] and Kehui Wu[1,2]

[1] *Institute of Physics, Chinese Academy of Sciences, Beijing 100190, China*

[2] *Collaborative Innovation Center of Quantum Matter, Beijing 100871, China*

Table of Contents

1. 2D boron grown on Ag(111) under different substrate temperatures

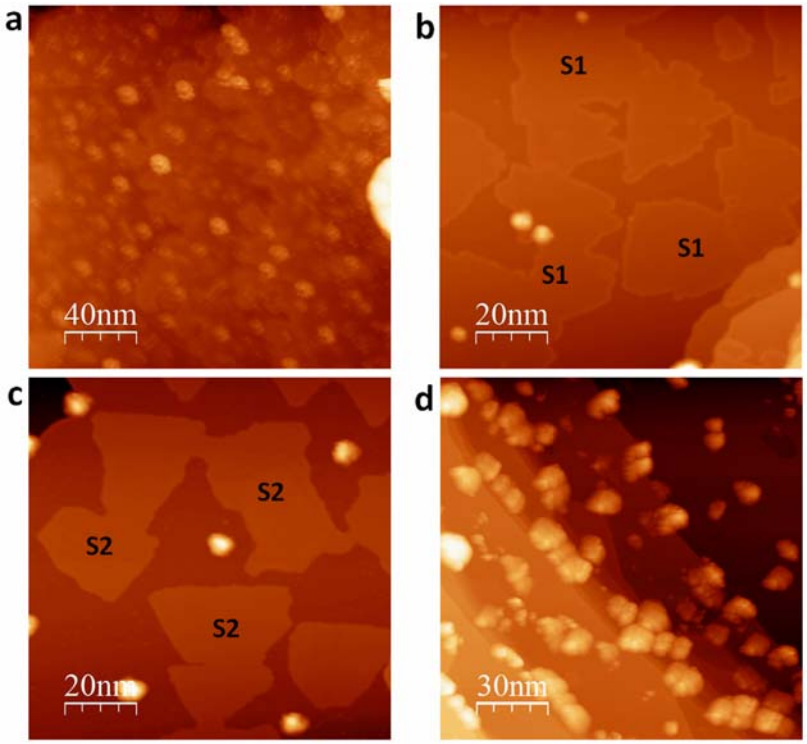

Supplementary Figure 1 Scanning tunneling microscopy (STM) images taken on the 2D boron on Ag(111) surface under different substrate temperatures (T) during growth. (a) T = 300 K; (b) T = 570 K; (c) T = 700 K; (d) T = 870 K. Scanning parameters: (a) 200×200 nm^2, V_{tip}= -3.9 V; (b) 100×100 nm^2, V_{tip}= -3.9 V. (c) 100×100 nm^2, V_{tip}= -3.5V, I = 200 pA. (d) 100×10 0nm^2, V_{tip}= -3.9 V. (c) 150×150 nm^2, V_{tip}= -3 V.

In our experiments, we found the formation of 2D boron on Ag(111) is strongly dependent on the substrate temperature during growth. When the temperature was below 500 K, only clusters or disordered structures form on the surface, which is shown in Supplementary Fig. 1(a). If the substrate temperature is above 550 K, 2D boron islands of S1 phase are observed (Supplementary Fig. 1(b)). The S1 phase can be transformed to S2 phase when annealing the sample with S1 phase to above 650 K. On the other hand, the S2 phase can also been obtained by directly growing boron on Ag(111) surface with substrate temperature higher than 650 K, and the STM image is shown in Supplementary Fig. 1(c). Increasing substrate temperature to above 850 K, only 3D clusters form on surface (Supplementary Fig. 1(d)).

2. Charge distribution in 2D boron structures

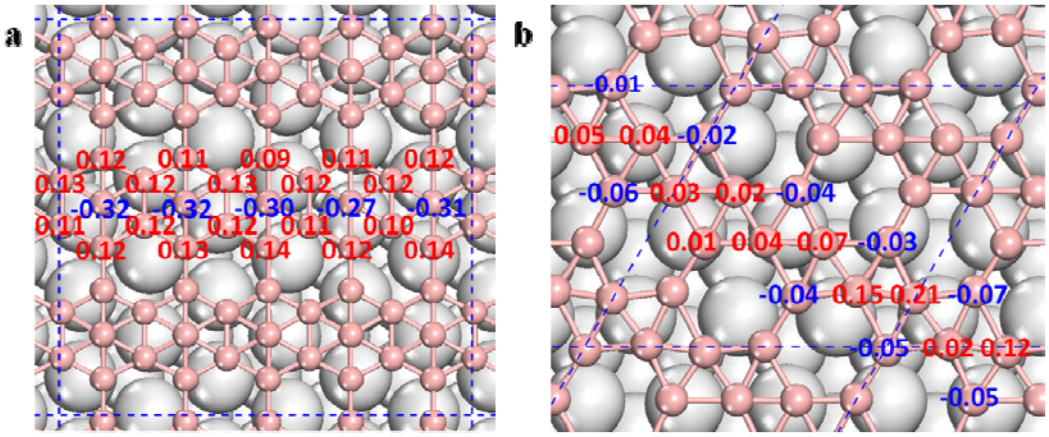

Supplementary Figure 2 Calculated partial charges of boron atoms in (a) S1 and (b) S2 sheets adsorbed on Ag(111) using the Bader analysis based on electron densities. The pink and green balls represent boron and silver atoms, respectively.

The charge distributions on boron atoms in 2D boron sheet are important, as it is strongly relevant to the explanation of scanning tunneling microscopy (STM), scanning tunneling spectroscopy (STS), and x-ray photoelectron spectroscopy (XPS) data. Based on Bader's charge analysis, the atomic charges of 2D boron (S1 and S2 phases) are obtained, as shown in Supplementary Fig. 2. In the S1 phase (Supplementary Fig. 2(a)), the B atoms at the centers of the hexagonal boron ribbons are negatively charged (~ -0.3 electron), and B atoms surrounding the holes are positively charged (~ 0.1 electron). Similarly, asymmetric charge distribution is also found in the S2 phase, as shown in Supplementary Fig. 2(b). Atoms in some regions of boron rows have larger positive charge (~ 0.2 e) than other regions (~ 0.0 e). This would lead to dark-bright alteration in the STM image of the S2 phase, as observed experimentally.

Such inhomogeneous charge distributions are due to different B-Ag interactions at different adsorption sites of boron on Ag(111). Additionally, the coexistence of negative and positive charged atoms in 2D sheets indicates boron atoms have different chemical environments, corresponding to the two pristine B-B peaks for the B 1s signal in XPS.

3. Boron growth on Ag(111) with increasing coverage

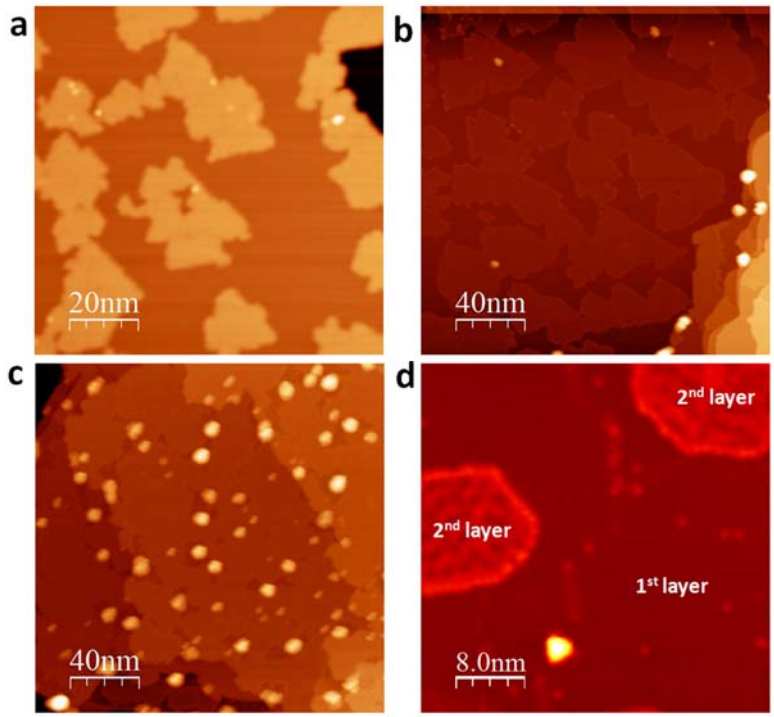

Supplementary Figure 3 STM images taken on the 2D boron on Ag(111) surface with various coverages: (a) about 50%; (b) about 80%; (c) about 95%. Scanning parameters: (a) 100×100 nm^2, V_{tip}= -3.0V; (b) 200×200 nm^2, V_{tip}= -3.9 V. (c) 200×200 nm^2, V_{tip}= -3.8V. (d) 40×40 nm^2, V_{tip}= -2.0V. It is noted that there are several steps on the bottom right of image (b). But these steps are Ag(111) steps, not multilayer boron sheet.

We have studied the coverage dependence of 2D boron growth on Ag(111) surface, as shown in Supplementary Fig. 3. It is found that with increasing boron coverage, the size of 2D boron islands increases until they percolate to form an almost completed monolayer (ML) film. It is also noted that when B coverage is close to 1 ML, 3D clusters start to form on the surface (Supplementary Fig. 3(c)). We only occasionally observed some small islands of second layer of boron on top of first layer (Supplementary Fig. 3(d)), which exhibit a different structure from first layer. The formation of 3D clusters is the result of the saturation of the Ag-B interfacial interactions when the first layer completely forms. This also implies the interfacial interactions should play an important role in the formation of 2D boron sheets.

4. B coverage calibration

It is previously reported the well-known Si(111)-(√3×√3)R30º-B structure can form when boron is deposited on Si(111) and annealed to above 700°C, [1]. The boron atoms are located at the S_5 sites, *i.e.*, boron is directly underneath a silicon adatom, leading to the corresponding protrusions darker in STM observation. The amount of B atoms can be obtained by counting the dark protrusions in STM images. The annealing temperature is below 900°C to avoid B atom diffusion into the bulk of Si(111) [2]. Based on this method, we can precisely determine the depositing boron flux.

Supplementary Fig. 4 shows two experiments with different B flux. In the first experiment, we grow boron on Ag(111) for 10 minutes at substrate temperature of 570 K. After that, the substrate is switched to Si(111) immediately and the B is grown on Si(111) for 2 minutes at room temperature. During the whole growth process, the B flux is monitored to maintain constant. Then the B/Si(111) sample is annealed to approximately 1000 K to form Si(111)-(√3×√3)R30º-B structure. The prepared B/Si(111) and B/Ag(111) samples are then scanned by STM separately. In Supplementary Fig. 4(a) and 4(b), we show typical STM images of B/Si(111) and B/Ag(111), respectively. The density of B atoms on Si(111) is determined to be 1.82±0.05 nm^{-2} based on statistical analysis of a large number of STM images. On Ag(111), the coverage of S1 can be determined as 27.2±1.4% by measuring more than twenty STM images at different locations. Therefore, the B density in the S1 phase can be determined to be 33.6±2.0 nm^{-2}, greatly agreeing with the theoretical model of 34.48 nm^{-2}.

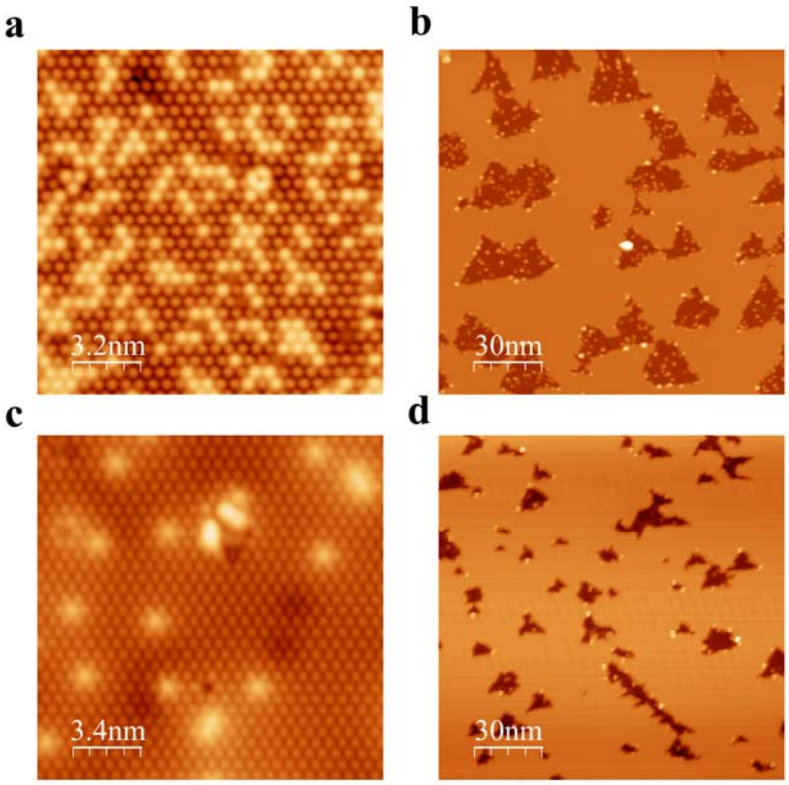

Supplementary Figure 4 (a, c) STM images of B on Si(111). (b, d) STM images of B on Ag(111). For (a) and (b), the flux of B is the same, but the growth time is different, i.e. 2 minutes for (a) and 10 minutes for (b). For (c) and (d), both the flux and growth time are the same.

In the second experiment, the growth time of boron on both Ag(111) and Si(111) was set to 5 minutes. So in this case the density of boron atoms on two surfaces should be same. Typical STM topographic images of B/Si(111) and B/Ag(111) are shown in Supplementary Fig. 4(c) and 4(d). Similar analysis give the density of B atom as 2.6±0.05 nm^{-2} on Si(111) and 2.67±0.50 nm^{-2} on Ag(111). This result also proves the validity of our structure model.

5. Air exposure of 2D boron

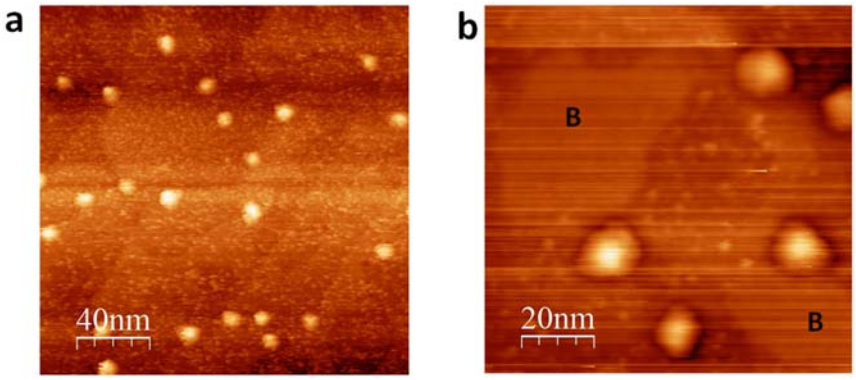

Supplementary Figure 5 STM images taken on the 2D boron on Ag(111) surface which were first exposed to air and then transferred back into UHV chamber: (a) without degas. (b) with degas at 350K. Scanning parameters: (a) 200×200 nm^2, V_{tip}= -4.0 V; (b) 100×100 nm^2, V_{tip}= -5.0 V.

To probe the stability of the 2D boron sheets exposed to air, we prepare a sample of the S1 phase and expose it to air for about 10 min, and then transfer it back to the UHV chamber for STM observations. The initial coverage of 2D boron islands is ~ 0.5 ML. After air exposure, the surface becomes featureless and filled with clusters formed by air contaminations (Supplementary Fig. 5(a)). After degassing this sample at 350 K, some smooth areas on terraces are recovered, while the rest part of the surface still remains featureless (Supplementary Fig. 5(b)). Considering that the Ag(111) surface is easy to be oxidized in air, we suggest that the smooth area corresponds to the 2D boron sheets, which could be partially recovered after degassing, and the featureless area corresponds to oxidized Ag(111) surface.

6. Oxidization of 2D boron

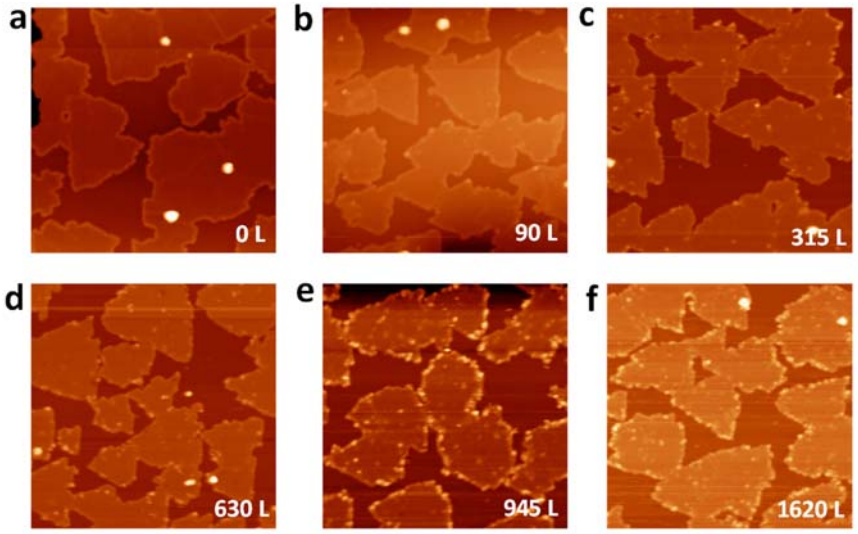

Supplementary Figure 6 STM images of 2D boron sheets on Ag(111) surface after oxygen gas dose of (a) 0 L, (b) 90 L, (c) 315 L, (d) 630 L, (e) 945 L, and (f) 1620 L. Scanning parameters of all the STM images are: 100 × 100 nm2, Vtip= -4.0 V, I = 200 pA.

As the exposure of our sample in air generally results in dirty surfaces, we perform more controllable oxidation of our 2D boron sheets in UHV. The sample is exposed to oxygen gas which is introduced into our UHV chamber with different doses (up to 1600 Langmuir (L), 1 Langmuir = 1×10^{-6} torr.s), and the results are shown in Supplementary Fig. 6. It is hardly found any sign of oxidation for oxygen dose below 300 L. When the oxygen dose increases to 945 L, there are increasing bright spots occurring at the edges of boron sheets, while the terraces of boron sheets remains intact. Continuing to increase oxygen dose up to 1620 L, the STM image shows no much change. The terraces keep flat and the stripe features of S1 are still the same. This experiment indicates that the B atoms inside the 2D boron sheets are quite inert to oxidation. It is why the ratio of oxidized to unoxidized boron atoms is quite small (0.23) even for boron sheets exposed to air. This experiment also supports the conclusion that the oxidized boron atoms may come mostly from the edges of the sheets, while the body of the sheets remains intact.

7. Band structures of 2D boron sheets by DFT

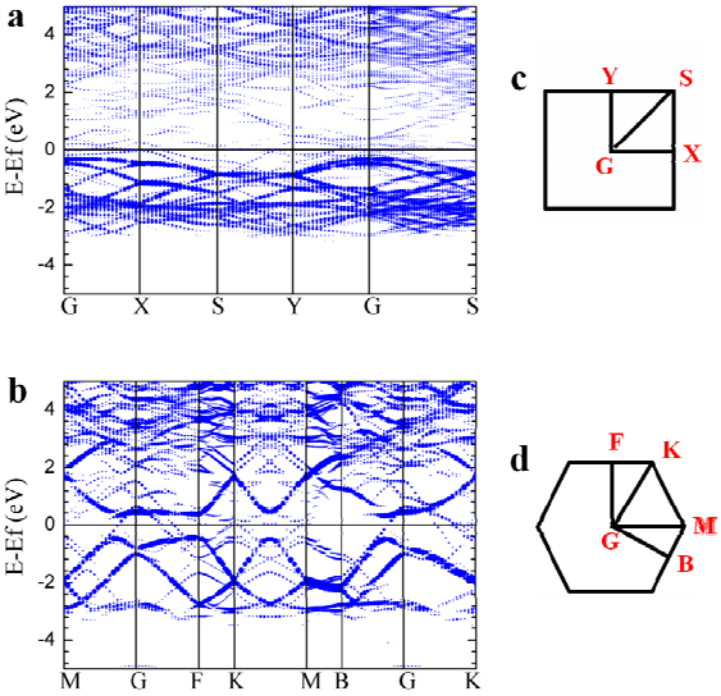

Supplementary Figure 7 Projected band structures of 2D boron sheets on Ag(111). (a, b) Band structures of S1 and S2, respectively. The size of blue dot denotes to the contribution weight. (c, d) The high symmetric points of the 2D Brillouin zones for S1 and S2, respectively.

The band structures of 2D boron on Ag(111) surface (Supplementary Fig. 7) and free-standing boron sheets (Supplementary Fig. 8) are calculated, which show both S1 and S2 phases are metallic.

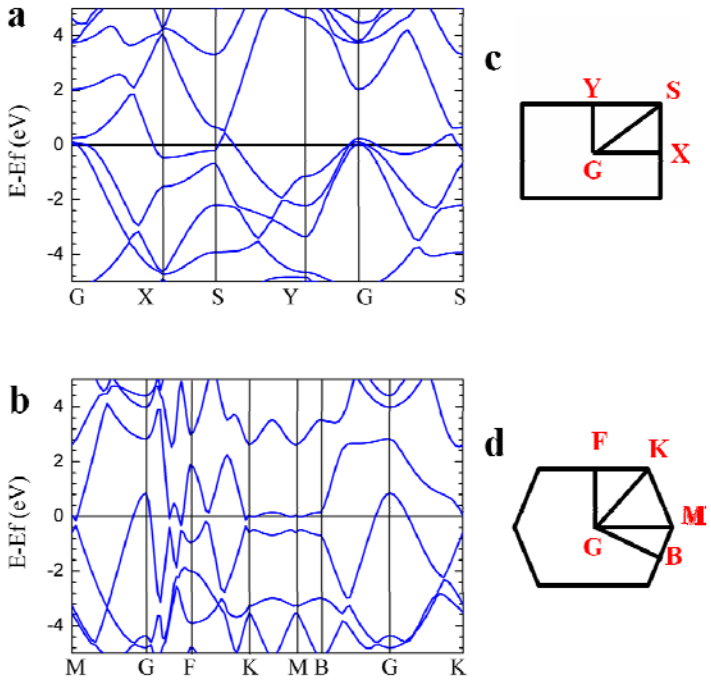

Supplementary Figure 8 Calculated band structure of freestanding 2D boron sheets. (a, b) Band structures of S1 and S2, respectively. (c, d) The high symmetric points of the 2D Brillouin zones for S1 and S2, respectively.

8. Electronic states of 2D boron sheets by STS

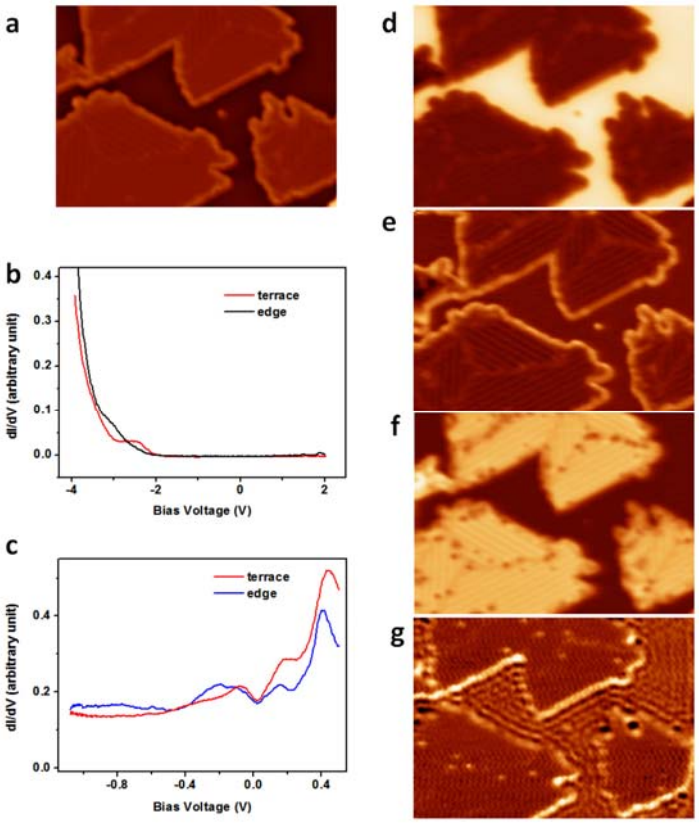

Supplementary Figure 9 (a) STM image taken on the 2D boron on Ag(111) surface. (b, c) dI/dV curves taken on the terrace and edge of 2D boron sheet with different energy ranges. (d-g) dI/dV maps of the same area as (a). Scanning parameters: (a) 60×43 nm^2, V_{tip}= -4.0 V; (d) 60×43 nm^2, V_{tip}= -4.0 V; (e) 60×43 nm^2, V_{tip}= -3.2 V; (f) 60×43 nm^2, V_{tip}= -2.5 V; (f) 60×43 nm^2, V_{tip}= -0.2 V.

STS probes the distribution of local density of states (LDOS) of the surface. We perform STS on 2D boron sheet on Ag(111), as shown in Supplementary Fig. 9. In the large bias voltage range, there is a prominent LDOS peak at -2.5 V (the STS of S1 and S2 are similar). The LDOS at energy range from -2V to +2V is quite low, which looks like there is a large gap about 4 eV (Supplementary Fig. 9(b)). However in the dI/dV curve taken at smaller bias voltage range (Supplementary Fig. 9(c)), there are still rich LDOS around the Fermi level, which indicates that our 2D boron is metallic. First-principles calculations give metallic band structure features of both the S1 and S2 phases (Supplementary Fig. 7), agreeing well with the STS observations. We also show the calculated DOS of S1 phase and S2 phase in Supplementary Fig. 10(a) and (b), and

found a prominent peak, mainly contributed by p-bands of boron, at -2.0eV (-2.5eV) for S1 (S2) phase, which accords with dI/dV curve very well. The DOS distribution around Fermi level shows that both structures are metallic.

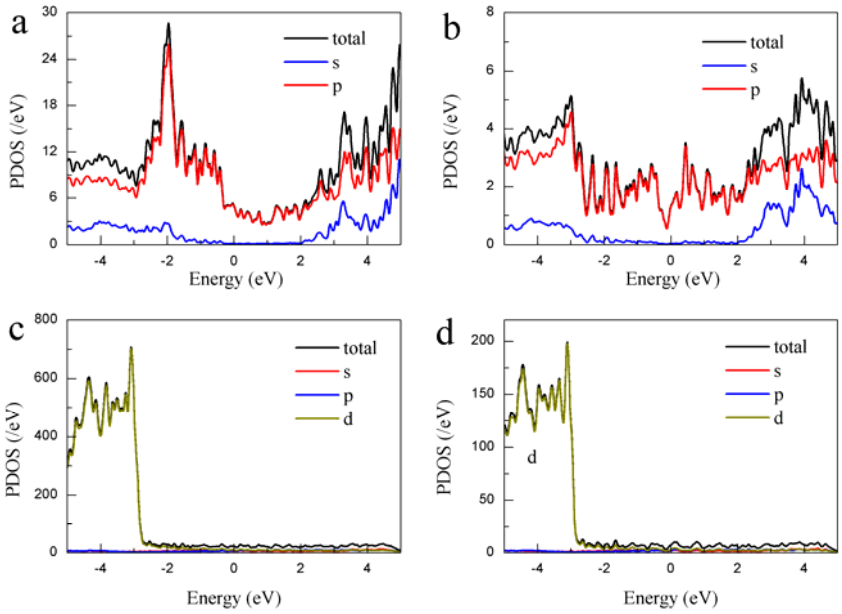

Supplementary Figure 10 Projected density of states (PDOS) for (a) S1 and (b) S2 sheets and their Ag(111) substrates (c, d), respectively.

9. Shapes of 2D boron islands

The S1 phase is characterized by the stripes running in three crystallographic orientations. Carefully examining Supplementary Fig. 11, one can find two kinds of islands for S1 phase: one has regular triangular shape, the other is relatively irregular. In the regular triangular islands, the edges are along the direction of stripes. In our structure model, the stripes are running perpendicular to the boron-row direction (*b* direction in Fig.2(a) in the main text or [1-10] direction of Ag(111)). This implies that cutting an edge along the *b* direction can result in a smooth island edge. In contrast, in most irregular islands the edges are running perpendicular to stripes (*a* direction in Fig.2(a) of paper or [-1-12] direction of Ag(111)), meaning that cutting the island along the *a* orientation usually result in irregular edges. In our experiment these two types of islands usually coexist with comparable coverage. This indicates that the energetic stabilities of two types of edges are quite close to each other. The straight edge of S1 along stripes may be related to the strain due to the slight mismatch between the 2D boron lattice and the Ag(111) lattice. The strain is accumulated along the boron row direction (*a*) with the increasing length, which is perpendicular to stripes. On the other hand, the S2 structure is much smoother than the S1 phase. There is no apparent stripe feature on the surface of S2 (Fig.1(b) of paper).

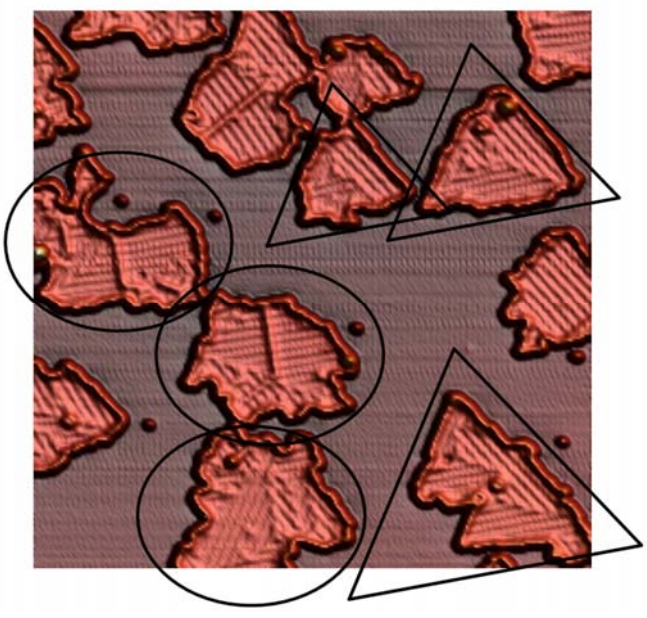

Supplementary Figure 11 3D version of Fig.1(a) in paper. The stripes can be observed more clearly. The black triangles and ellipses mark the triangular and irregular boron islands, respectively.

10. Edge states of 2D boron sheets

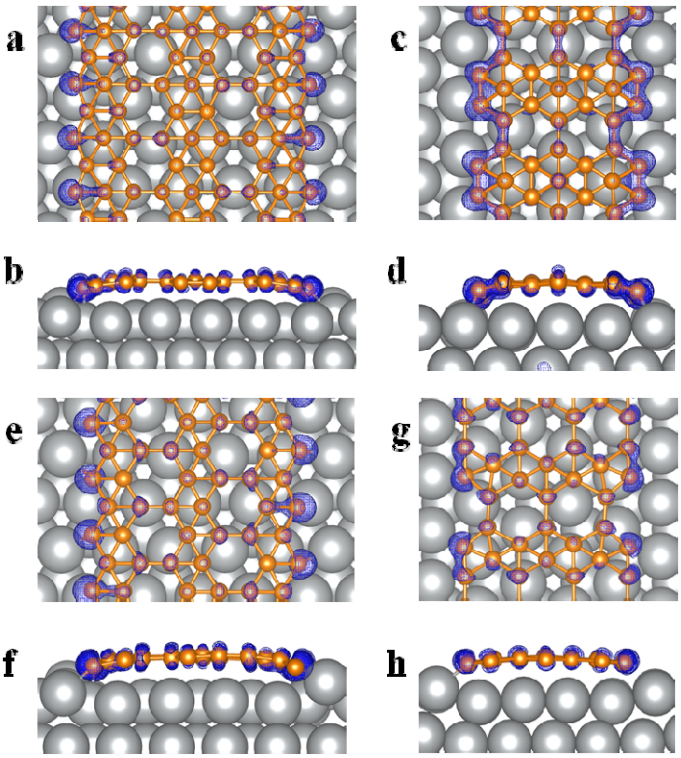

Supplementary Figure 12 Top and side views of spatial distributions of electron density in the vicinity of Fermi levels (±2.0 eV, isovalue = 0.03 e/Å^3). (a, b) S1 phase with zigzag edge, (c, d) S1 phase with armchair edge, (e, f) S2 phase with zigzag edge, and (g, h) S2 phase with armchair edge, respectively. Display style: Ag atoms in big grey balls, B atoms in small orange balls, electron density in blue cubes.

The STM image shown in Supplementary Fig. 9(a) reveals that the edges of 2D boron islands are brighter than the island surface, suggesting the existence of edge states. To study this issue, we performed systematic dI/dV measurements and STS mapping. The dI/dV curves (Supplementary Fig. 9(b) and (c)) on edges show additional shoulders around -3.0 eV and -0.2 eV, and the dI/dV maps at -3.2 eV and -0.2eV (Supplementary Fig. 9(e) and (g)) also show the brighter edges, indicating the existence of edge states. According the atomic model of S1 phase, the straight edge is armchair-like, while another is zigzag-like (Supplementary Fig.12). To figure out the origin of the edge states, we perform DFT calculation on four kinds of 2D boron nanorribons: (a) S1 with

zigzag edge, (b) S1 with armchair edge, (c) S2 with zigzag edge, and (d) S2 with armchair edge. The optimized structures reveal that all the edges of S1 and S2 ribbons are bonded to the Ag(111) substrate (Supplementary Fig.12), as the distances between the B atoms at edge and the Ag(111) substrate are significantly shorter than the interlayer distance between 2D boron and substrate, which can result in B-Ag hybrid states in the vicinity of the Fermi level. We further plot the distributions of electron density in the energy range of -2.0 ~ 2.0 eV with respect to the Fermi levels, as shown by the blue cubes in Supplementary Fig.12. It is found that both the zigzag and armchair edges have much higher electron density than inner part of 2D boron, indicating that significant edge states.

11. Height of 2D boron sheets

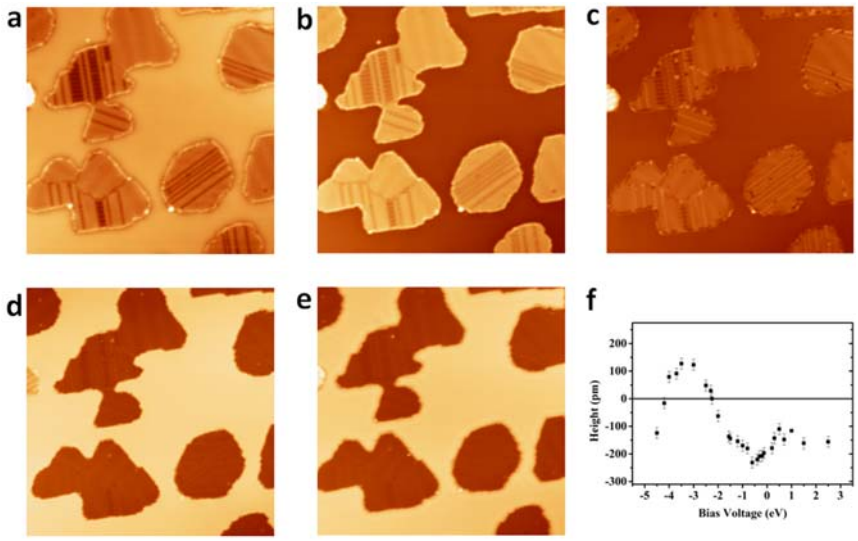

Supplementary Figure 13 (a-e) STM images of the same area as that of Fig.1(d) of the paper. The bias voltages are (a) -4.2 V, (b) -4.0 V, (c) -2.3 V, (d) -1.0 V, (e) 1.5 V, respectively. (f) The height of the 2D boron sheet as a function of tip bias.

In STM, the tunneling current depends strongly on the local density of states (LDOS) of a surface, and therefore the measured height of a surface step is valid only when the upper terrace and the lower terrace have the same LDOS, i.e. they are the same material. In the case of boron island on Ag(111) surface, the LDOS is quite different for the boron sheet and the Ag(111) surface. As a result the measured height of the boron island drastically depends on the STM bias voltage. For example, we show a series of STM images of the same area of with different tip bias voltages (Supplementary Fig. 13(a)-(e)). The 2D boron islands are higher than surrounding Ag(111) terrace with bias voltage between -2.3 V and -4.1 V, while at other voltages the 2D boron appear lower than the Ag(111) terrace (Supplementary Fig. 13(f)). The bias-dependent height demonstrates the strong influence of DOS on the height measurement by STM.

The relative height of the 2D B sheet with respect to the Ag(111) substrate can be qualitatively understood as follow. The dI/dV curve obtained on 2D boron surface shows a prominent peak at about -2.5 V with FWHM about 0.5 V (Supplementary Fig. 9(b)), while LDOS around the Fermi level is quite low. On the other hand, there is a well-known surface state near Fermi level in

Ag(111) surface. In STM measurement, the tunneling current reflects the integration of LDOS of sample. As a result, the 2D boron islands appear lower than surrounding Ag(111) terrace at bias voltage near Fermi level, and higher than Ag(111) at high bias voltages.

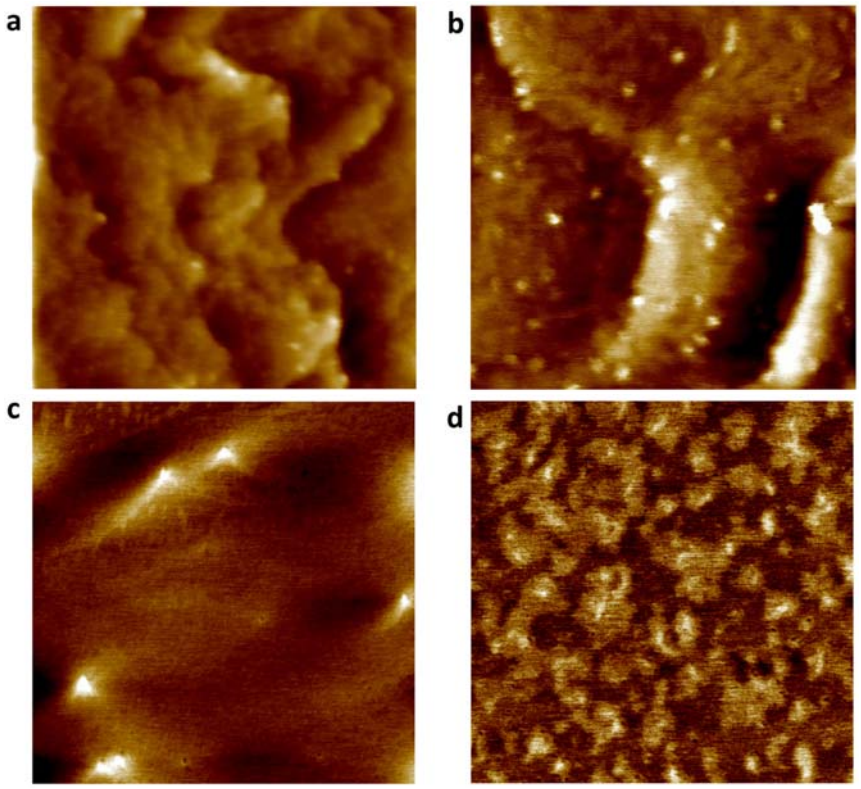

Supplementary Figure 14 (a, b) AFM images taken on the 2D boron on Ag(111) surface in air. (c, d) AFM images taken on Ag(111) surface in air. (a) 1000×1000 nm^2; (b) 330×330 nm^2; (c) 1000×1000 nm^2; (d) 500×500 nm^2 .

Atomic force microscopy (AFM) measurement may also provide information on the thickness of the boron sheet. Usually, AFM measurement can provide the step height of many single crystal substrates, such as oxides. However, for metal surface such as Ag(111) that is easy to be oxidized in air, a measurement of single step and terrace on the surface is generally not feasible, We performed AFM measurements on the 2D boron sheets on Ag(111) surface in air, and the results are shown in Supplementary Fig. 14(a) and (b). The surface is rough, and we cannot observe monolayer steps or terraces. We believe that this is due to the oxidation of the Ag(111) surface which is not covered by boron. To prove this, we performed AFM measurements on a pure Ag(111)

surface (without boron deposition), and the results are shown in Supplementary Fig. 14(c) and (d). We found the surface exhibits similar rough and contamination features, and monolayer steps are not observable. So it is impossible to obtain the information on the thickness of the boron sheet by AFM measurements in air. Note that with the same AFM system we were able to obtain monolayer step/terrace morphology of many semiconductor and oxide surfaces.

12. XPS data of Ag 3d signal

Supplementary Fig. 15 shows the Ag 3d signal of XPS. As the Ag(111) surface is metallic, asymmetric Gaussian-Lorentzian is employed to fit the peaks. The fitting results of peak positions are 368.2 eV and 374.2 eV, and there is no obvious splitting of both peaks. The positions of the two peaks are consistent to the value of pure Ag: 368.3 eV and 374.3 eV. Especially, the distance between the two peaks is the same with that of pure Ag. The small shift of the whole spectrum towards the Fermi level may originate from the systematic error in different machines. We suggest that the predominant signal of Ag come from the substrate underneath the surface. Due to the strong background, it is difficult to see any signal even if the Ag atoms at the surface do have some interaction with boron atoms to change their chemical state. On the other hand, since all B atoms are on the surface, the change of the chemical state of boron atoms is easier to detect by XPS.

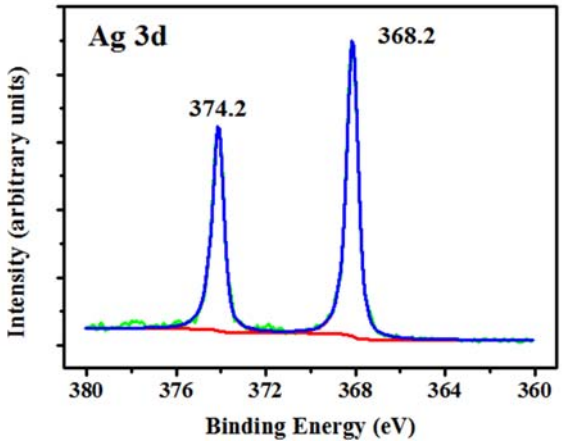

Supplementary Figure 15. Ag 3d signals of XPS of boron sheets on Ag(111) with boron coverage 1 ML. The peaks were fitted using combined Gaussian-Lorentzian function. The ratio of Lorentzian function is fixed to be 45% and 55% for 368.2 and 374.2 eV peaks respectively. We subtracted a Shirley background in peak fitting. The green, red and blue curves correspond to original data, fitting lines, sum of fitting lines, respectively.

References:

[1] Bedrossian, P., Meade, P. D., Mortensen, K., Chen, D. M., Golovchenko, J. A. & Vanderbilt, D. *Phys. Rev. Lett.* 63, 1257(1989).

[2] Cao, Y., Yang, X. & Pianetta, P. *J. Vac. Sci. Technol. A* **11**, 1817(1993).